

# Synthesis, Comparative Characterization and Photocatalytic Application of SnO<sub>2</sub>/MWCNT Nanocomposite Materials

Z. Nemeth<sup>1</sup>, Z. Pallai<sup>1</sup>, B. Reti<sup>1</sup>, Z. Balogh<sup>2</sup>, O. Berkesi<sup>3</sup>, K. Baan<sup>3</sup>, A. Erdohelyi<sup>3</sup>, E. Horvath<sup>4</sup>, G. Veréb<sup>5</sup>, A. Dombi<sup>5</sup>, L. Forró<sup>4</sup> and K. Hernadi<sup>1,5,\*</sup>

<sup>1</sup>Department of Applied and Environmental Chemistry, University of Szeged, H-6720 Szeged, Hungary

<sup>2</sup>Center for Electron Nanoscopy, Technical University of Denmark, DK-2800 Lyngby, Denmark

<sup>3</sup>Department of Physical Chemistry and Material Science, University of Szeged, H-6720 Szeged, Hungary

<sup>4</sup>Laboratory of Physics of Complex Matter, École Polytechnique Fédérale de Lausanne, CH-1015 Lausanne, Switzerland

<sup>5</sup>Research Group of Environmental Chemistry, Institute of Chemistry, University of Szeged, H-6720 Szeged, Hungary

**Abstract:** Two different preparation methods were developed to cover successfully multi-walled carbon nanotubes (MWCNT) with tin-dioxide (SnO<sub>2</sub>) nanoparticles using SnCl<sub>2</sub>·2H<sub>2</sub>O as precursor under different solvent conditions. The applied mass ratios of the components were 1:4, 1:8, 1:16, 1:32 and 1:64, respectively. As-prepared tin-dioxide coverages were characterized by TEM, SEM, SEM-EDX, Raman microscopy, BET and X-ray diffraction techniques. Photocatalytic efficiencies of selected composites were investigated in a self-made photoreactor, equipped with UV-A fluorescence lamps. Photocatalytic degradation of phenol solution was followed by using HPLC. Observations revealed that using hydrothermal method we can easily control the layer of SnO<sub>2</sub> nanoparticles on the surface of MWCNTs. Using various solvents SnO<sub>2</sub> nanoparticles with different morphologies formed. The nanocomposites have low photocatalytic efficiencies under conditions used generally (when λ > 300 nm).

Received on 19-09-2014  
Accepted on 17-10-2014  
Published on 30-10-2014

**Keywords:** Carbon nanotubes, chemical synthesis, electron microscopy, IR spectroscopy, photocatalysis.

## 1. INTRODUCTION

Due to their excellent mechanical, physical and unique electronic properties, carbon nanotubes (CNTs) have attracted worldwide attention since they were discovered [1]. CNTs are considered as promising candidates for many applications such as composite materials [2], field emission materials [3] or chemical sensors [4]. The combination of CNTs and nanoparticles are expected to deliver exceptional performances in solar cells, catalyst and nanoelectric devices [5-8]. It is well known that carbon nanotubes can provide a desirable electronic matrix for anode materials due to their high theoretical electrical conductivity, high aspect ratio and good mechanical properties [9].

There have been several recent investigations concerning the attachment of various inorganic compounds onto single-walled (SWCNTs) and multi-walled CNTs (MWCNTs) such as

SnO<sub>2</sub> [10-16] using different preparation techniques. MWCNTs were coated with SnO<sub>2</sub> by chemical solution method in which acid-treated MWCNTs was needed [17]. Zhu *et al.* [18] reported MWCNT/SnO<sub>2</sub> core-shell structures prepared by a double coating process in a wet chemical route. Du *et al.* synthesized SnO<sub>2</sub> nanotubes on carbon nanotubes by a layer-by-layer technique [19]. In some preliminary experiments, it has been observed that SnO<sub>2</sub> nanoparticles could be coated onto MWCNTs fully to form uniform layer by chemical vapour deposition [14]. In our previous papers, we successfully prepared SnO<sub>2</sub>/MWCNT nanocomposite by sol-gel method and investigated the gas sensor properties of the samples [20, 21].

As one of the most important semiconductor oxide, SnO<sub>2</sub> has been studied using for photocatalyst [22, 23]. SnO<sub>2</sub> have low photocatalytic efficiency due to its wide-bandgap (E<sub>g</sub> = 3.6 eV) and high recombination rates of photogenerated electron-hole pairs. These defects hinder the practical application of SnO<sub>2</sub> photocatalyst [24]. To overcome these problems, the fabrication of nanocomposites provides an

\*Department of Applied and Environmental Chemistry, University of Szeged, H-6720 Szeged, Hungary; Tel: +36 62 544 626; Fax: +36 62 544 619; E-mail: hernadi@chem.u-szeged.hu

effective way. On the other hand MWCNTs could be considered as a good electron acceptor for its unique structure [25]. Owing the unique features, it can serve as a good template of photocatalyst. The photoexcited electron will transfer from semiconductors to MWCNTs when the photocatalytic semiconducting oxides are coated on MWCNTs. The transfer prohibits the recombination rates of electron-hole pairs. This offers a feasible way to improve the photocatalytic efficiency [26].

Here, we present simple and cheap one-step methods, which provide SnO<sub>2</sub>/MWCNT composite materials in a controllable way with a different morphology and thickness of SnO<sub>2</sub> layer. The thickness of the coating can be easily controlled by change the concentration of reactant and solutions. The aim of this work is to present a comparative study for these synthesis techniques and the photocatalytic activity of the as-prepared SnO<sub>2</sub>/MWCNT nanocomposites materials.

## 2. EXPERIMENTAL

### 2.1. Materials

MWCNT were prepared by the decomposition of acetylene (CVD method) in a rotary oven at 720°C using Fe,Co/CaCO<sub>3</sub> catalyst [27]. This growth procedure using CaCO<sub>3</sub> catalyst enables a highly efficient selective formation of clean MWCNTs, suitable for effective bonding between MWCNT and precursors, without any amorphous carbon or carbonaceous particles [28]. Figures 1a and 1b show SEM image and Raman spectrum for pristine MWCNT. The spectrum shows strong peaks at 1342.7 cm<sup>-1</sup>, 1572.2 cm<sup>-1</sup> and 2680.1 cm<sup>-1</sup> which corresponds of the D, G and G' modes. There are also weak second-order peaks at 2443.9 cm<sup>-1</sup>, 2917.3 cm<sup>-1</sup> and 3220.0 cm<sup>-1</sup>. The intensity ratios between the main three peaks ( $I_D/I_G=0.52$ ,  $I_{G'}/I_G=0.7$  and  $I_G/I_D=1.35$ ) indicates good sp<sup>2</sup> structure and confirms the high-quality of multiwall carbon nanotube [29]. Following precursor molecule was used: SnCl<sub>2</sub>·2H<sub>2</sub>O (Molar

Chemicals). Solvents such as H<sub>2</sub>O, ethanol (ethanol was HPLC grade from Reanal) were applied.

### 2.2. Preparation of Composite Materials

#### 2.2.1. Impregnation

Firstly, 50 mg of clean MWCNTs were dispersed well in 50 cm<sup>3</sup> of the chosen solvent *via* sonication. In the next, step calculated amount of SnCl<sub>2</sub>·2H<sub>2</sub>O was dissolved in 20 cm<sup>3</sup> ethanol or water. For complete dissolution of the precursor compound 1 cm<sup>3</sup> cc. HCl was added to each of the suspensions. Finally, the solutions of the precursor were added to the MWCNT suspensions and sonicated for 30 min. After sonication, the mixture was heated to evaporate ethanol and water on a magnetic stirrer and dried at 110°C for 4 hours. The final mass ratios of MWCNT:SnO<sub>2</sub> composites were 1:4, 1:8, 1:16 1:32 and 1:64, respectively. The prepared samples were annealed in a static furnace in air at 450°C for 3 hours.

#### 2.2.2. Hydrothermal Synthesis

50 mg of clean MWCNTs were dispersed well in 50 cm<sup>3</sup> ethanol or water *via* sonication. The required amount of SnCl<sub>2</sub>·2H<sub>2</sub>O was dissolved in 20 cm<sup>3</sup> of the same solvent and 3 cm<sup>3</sup> cc. HCl was added to the mixtures. These suspensions were mixed and sonicated for 30 min. Finally, the solutions were poured into autoclaves and put in a static furnace for 24 hours at 150°C. At the end of the hydrothermal synthesis all samples were filtered and dried at 110°C for 4 hours. The final mass ratios of MWCNT:SnO<sub>2</sub> composites were 1:4, 1:8, 1:16, 1:32 and 1:64, respectively. The prepared samples were annealed in a static furnace in air at 450°C for 3 hours in order to prepare the SnO<sub>2</sub>/MWCNT nanocomposites.

### 2.3. Sample Characterization

In order to verify the formation of the inorganic coverage on the surface of MWCNTs, the resulted powder was investigated with transmission electron microscopy (TEM -

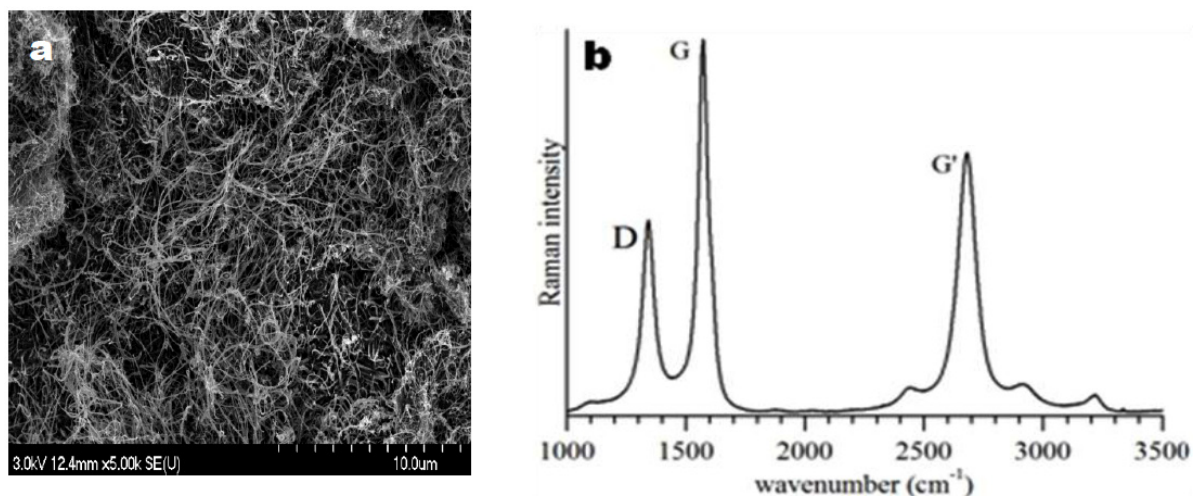


**Figure 1:** (a) SEM micrograph of pristine MWCNTs. (b) Raman spectra of MWCNT.

Philips CM 10) and high resolution transmission electron microscopy (FEI Tecnai G<sup>2</sup> T20 HR-TEM). A small amount of sample was sonicated in 1,25 cm<sup>3</sup> of distilled water or ethanol. A few drops from this suspension were dribbled onto the surface of the grid (CF 200 Cu TEM grid). Scanning electron microscopy (SEM) was done on a Hitachi S-4700 Type II FE-SEM operating in the range of 5-15 kV. The samples were mounted on a conductive carbon tape. For the specific surface area measurement BEL Japan, Inc. BELCAT-A type machine was carried out at 77 K using pre-treatment of heating the samples at 150°C for 30 min in helium flow (50 cm<sup>3</sup>/min). The energy-dispersive X-ray spectroscopy measurement was completed with the scanning electron microscope and a Röntec XFlash Detector 3001 SDD device. The crystalline structure of the inorganic layer was also studied by powder X-ray diffraction – XRD – (Rigaku Miniflex II Diffractometer) method using Cu K $\alpha$  radiation. Raman spectroscopy measurement was done on a Thermo Scientific DXR Raman microscope with a 532 nm laser (5 mW). The FT-IR spectra were recorded on a Bio-Rad Digilab Division FTS65A/896 FT-IR spectrometer equipped with a DTGS detector and a Ge/KBr beam splitter, between 4000 and 400 cm<sup>-1</sup>, at 4 cm<sup>-1</sup> optical resolution. A Harrick's Meridian® Split Pea Single Reflection Diamond ATR accessory was used, so no sample preparation was required. The spectrometer was controlled by Win IR Pro v.3.3 (Bio-Rad Digilab Division) software, and the spectra were analyzed using GRAMS/AI v.7.0 (Thermo Galactic) software.

#### 2.4. Determination of Photocatalytic Efficiency

The applied UV photoreactor was an open Pyrex glass tube with double walls, surrounded by a thermostating jacket (T = 25.0°C). The tubular reactor was surrounded by six fluorescent lamps (*Vilber-Lourmat T-6L UV-A*, 6W power, radiation maximum at 365 nm). The radiation intensity was determined by ferrioxalate actinometry ( $I = 1.25 \pm 0.01 \times 10^{-5}$  einstein dm<sup>-3</sup> s<sup>-1</sup> in the photoreactor). The added amount of the photocatalyst was 1 g/L, and 0.1 mM phenol (Spektrum3D, 99.0 %) solution was used as model contamination. The suspension (100 mL) was sonicated before the photocatalytic experiments, and it was stirred by a magnetic stirrer during the irradiation. Dissolved oxygen concentration was maintained by bubbling air through the suspension. Changes in phenol concentration was followed using an *Agilent 1100 series HPLC* system equipped with Lichrospher RP 18 column, using a methanol/water mixture as the eluent (the detection wavelength was 210 nm).

### 3. RESULTS AND DISCUSSION

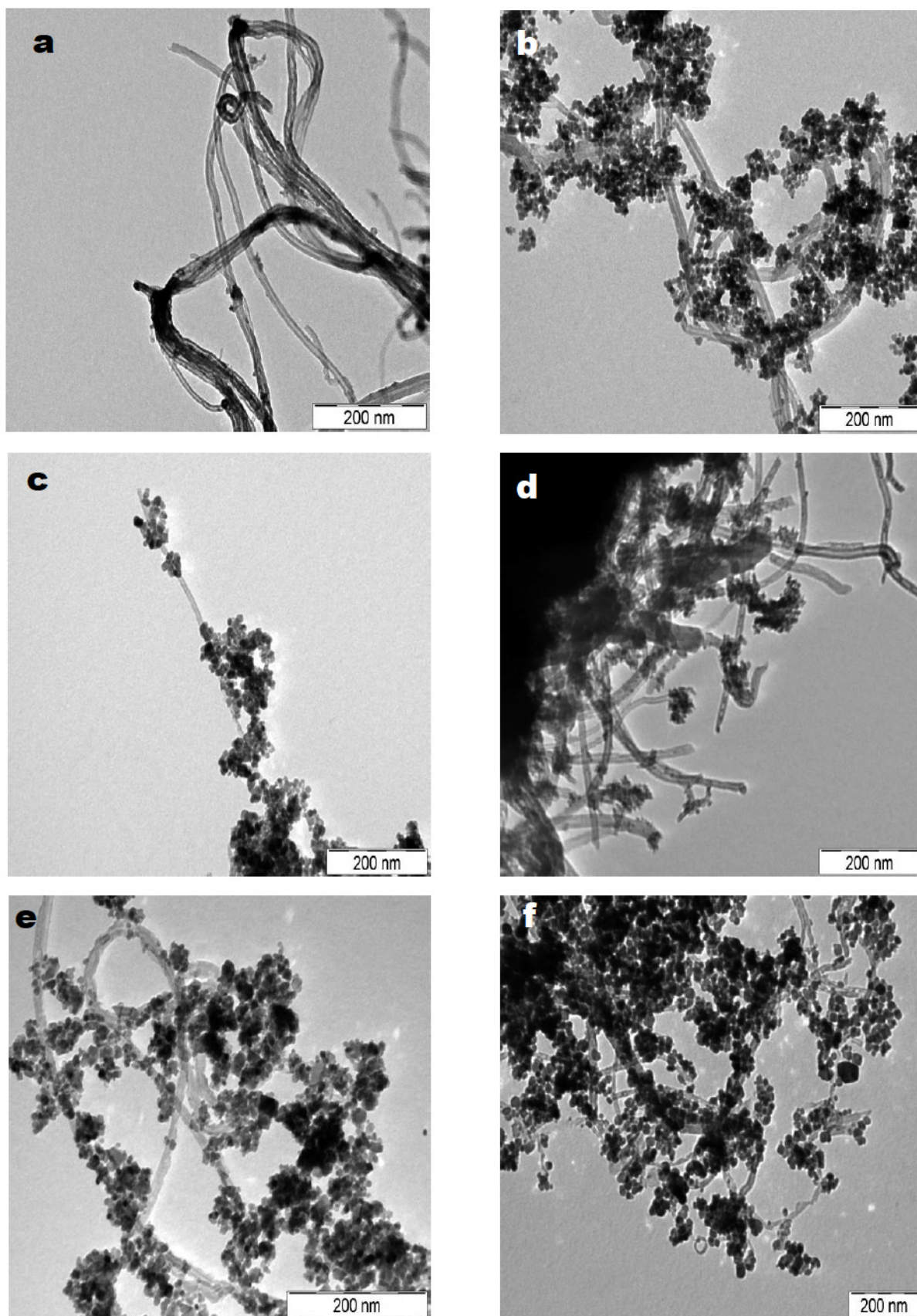
#### 3.1. Microscopic Analysis

After nanocomposite synthesis, samples were investigated by EM techniques. Production of SnO<sub>2</sub>/MWCNT nanocomposites was successful with both solvents. It has been found that samples with larger weight ratios are more favourable to

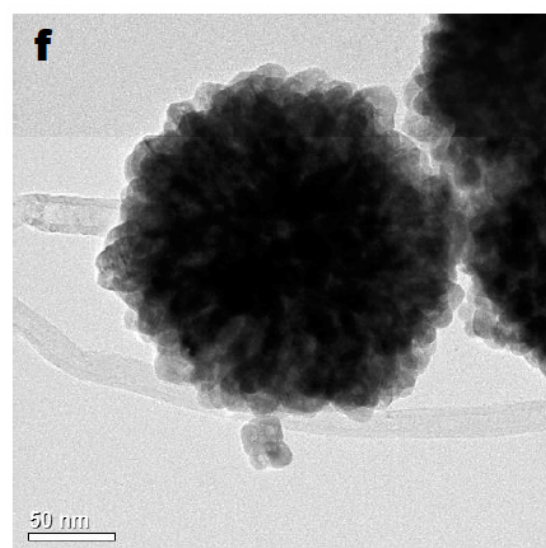
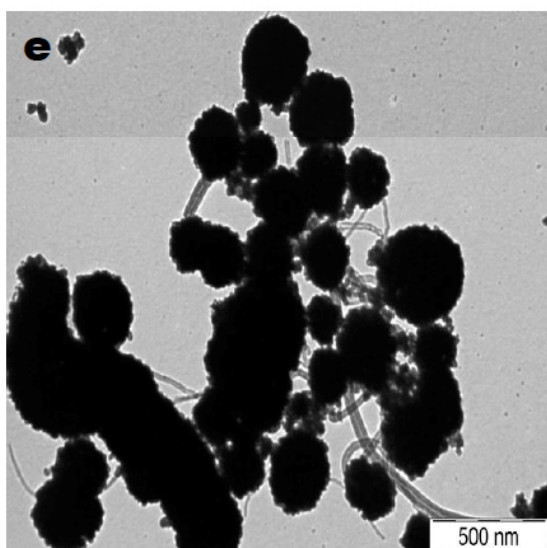
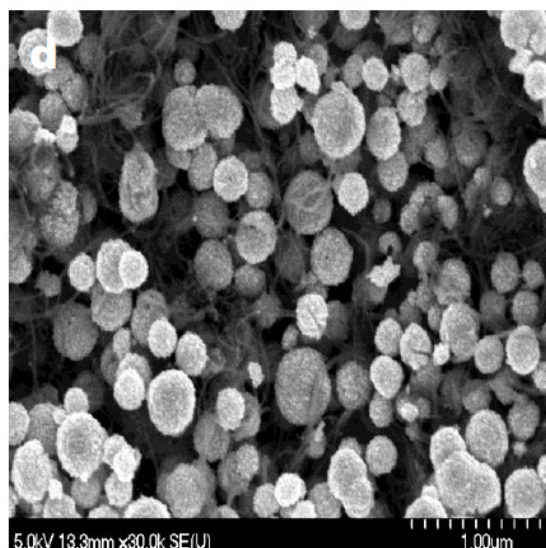
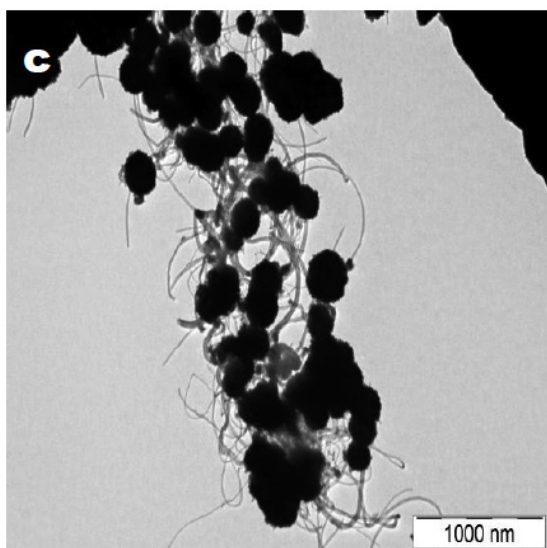
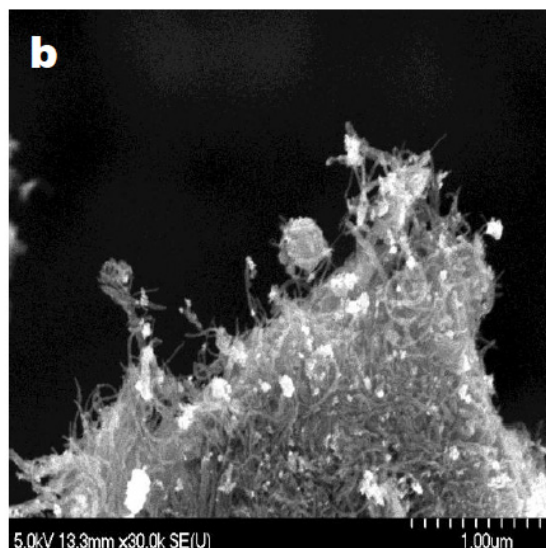
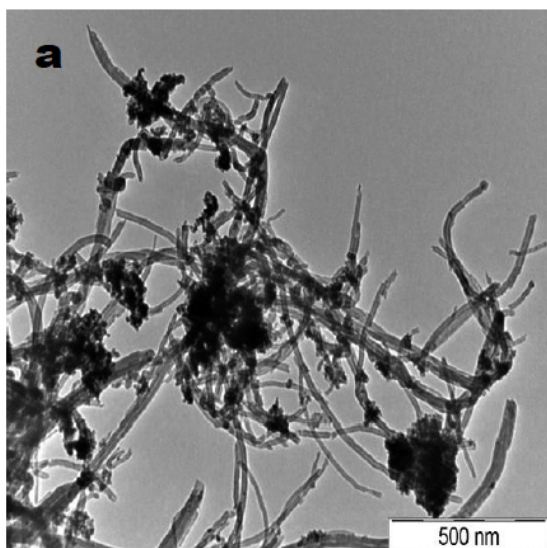
form interaction between SnO<sub>2</sub> nanoparticles and MWCNTs. In case of the 1:4 and 1:8 weight ratios, the samples mainly consisted of uncovered MWCNTs (Figure 2a). TEM observations revealed that increasing the quantity of the precursor increases the amount of SnO<sub>2</sub> nanoparticles adhered on the surface of MWCNTs using both solvents (Figures 2b-f). Based on the microscopic images we have not found significant difference between the morphology of the nanocomposites produced in H<sub>2</sub>O or EtOH medium.

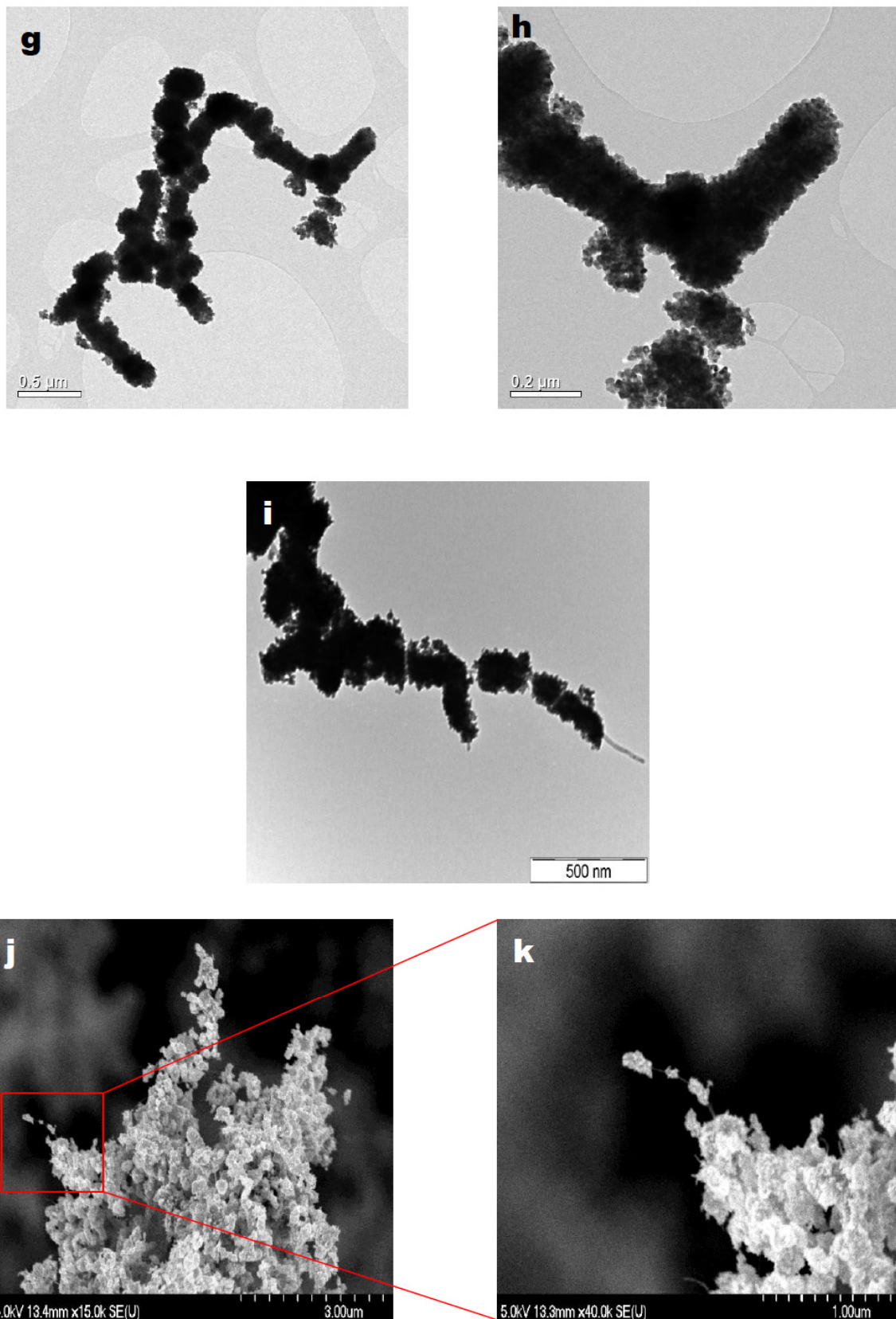
Analyzing the products from the hydrothermal synthesis reveals that this synthesis method provided more homogeneous and more uniform coverage. Although the resulting surface layers were different, the preparation of the nanocomposites was successful with both solvents. Figure 3 shows representative electron micrographs obtained from the composite materials prepared in ethanol. These EM images clearly demonstrated the presence of tin-dioxide layer on the surface of MWCNTs but the morphology is different. As can be seen in Figure 3, SnO<sub>2</sub> nanocrystallites were aggregated into bigger spherical crystallites in ethanol medium due to the surface tension of the solvent. In previously published results, SnO<sub>2</sub> crystallites with different morphologies can be observed by using different solvents, such as methanol, ethanol or water and applying hydrothermal synthesis [30, 31]. The surface tensions of these solvents are very different from each other, so the final morphology can be varied easily by changing the solvent [12].

Larger, segregated SnO<sub>2</sub> crystallites and uncovered MWCNTs were found when the weight ratio was 1:4 (Figures 3a and b). Applying higher weight ratios such as 1:8 and 1:16 TEM and SEM images clearly showed the adhered SnO<sub>2</sub> nanocrystallites on the surface of MWCNTs. These crystallites have spherical morphology due to the surface tension of ethanol and the assumed process of aggregation (Figures 3c-e). As can be seen in Figures 3f-k further increase in the concentration of tin-dioxide precursor the structure of the layer on the surface of MWCNTs was changed. In case of the 1:32 and 1:64 weight ratios the obtained nanocomposites consisted of almost completely covered MWCNTs (Figures 3f-k). TEM images in Figures 3f-h demonstrate more homogeneous surface coverage on the surface of MWCNTs when the mass ratio was 1:32. The shape of tin-dioxide crystallites presumably were also spherical, but in this case uniform surface coverage can be obtained and the SnO<sub>2</sub> nanocrystallites were not aggregated for each other probably due to the higher concentration of the precursor compound. The inorganic layer was partially broken into sections of e.g. 200 nm in length (Figures 3f and g). Larger SnO<sub>2</sub> nanocrystallites and thickly covered MWCNTs can be observed on SEM images (Figures 3j and k) when the weight ratio was 1:64. Analyzing the EM results segregated SnO<sub>2</sub> crystallites were found at this mass ratio. Consequently, the concentration of the precursor was too high for this sample.

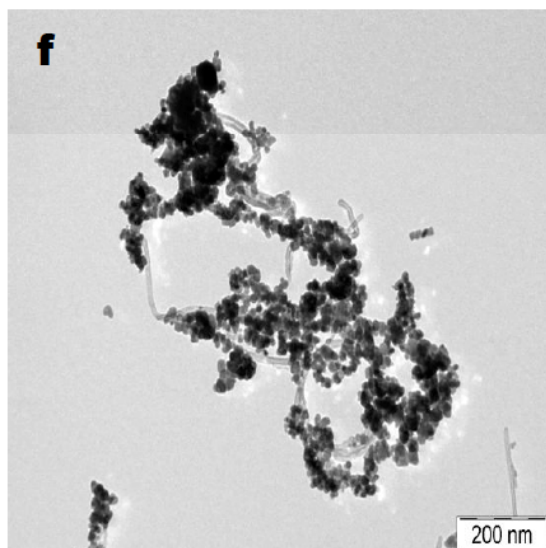
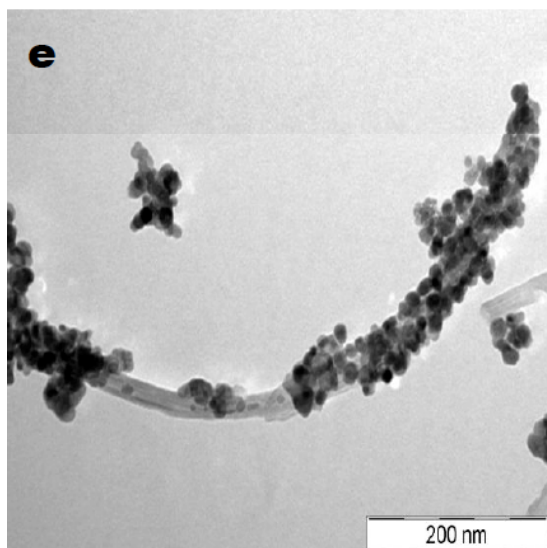
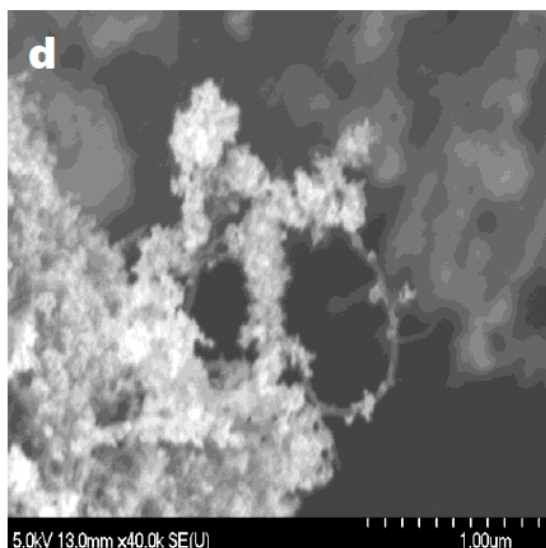
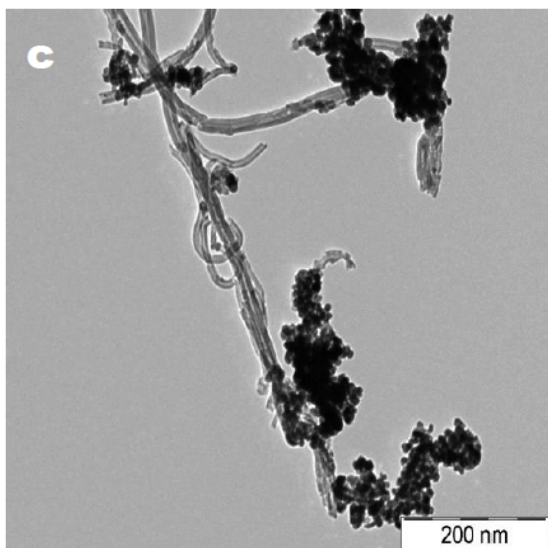
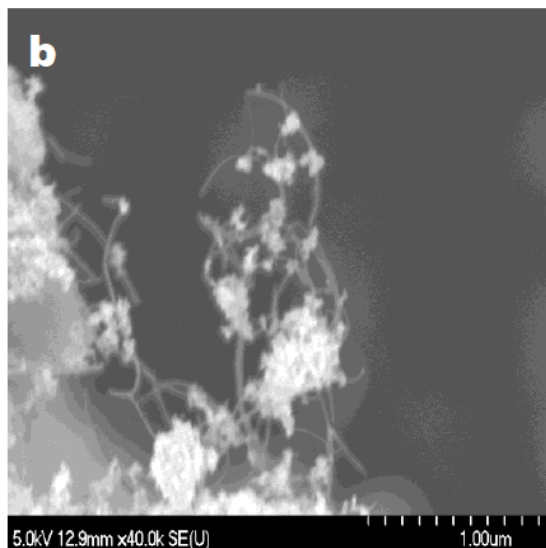
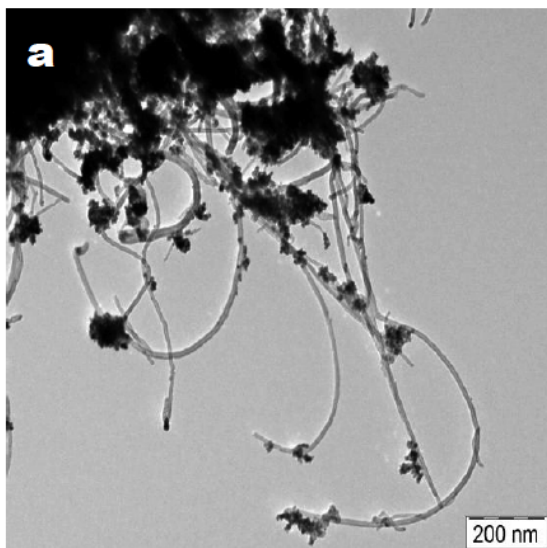


**Figure 2:** TEM images of composite fabricated by the impregnation technique. (a) prepared in water with MWCNT/SnO<sub>2</sub> ratio of 1:4. (b) prepared in water with MWCNT/SnO<sub>2</sub> ratio of 1:16. (c) prepared in water with MWCNT/SnO<sub>2</sub> ratio of 1:32. (d) prepared in water with MWCNT/SnO<sub>2</sub> ratio of 1:64. (e) prepared in EtOH with MWCNT/SnO<sub>2</sub> ratio of 1:16. (f) prepared in EtOH with MWCNT/SnO<sub>2</sub> ratio of 1:32.





**Figure 3:** TEM and SEM images of SnO<sub>2</sub>/MWNT nanocomposite prepared by the hydrothermal synthesis in EtOH. (a, b) with MWCNT/SnO<sub>2</sub> ratio of 1:4. (c, d) with MWCNT/SnO<sub>2</sub> ratio of 1:8. (e-f) with MWCNT/SnO<sub>2</sub> ratio of 1:16. (g-h) with MWCNT/SnO<sub>2</sub> ratio of 1:32. (i-k) with MWCNT/SnO<sub>2</sub> ratio of 1:64.



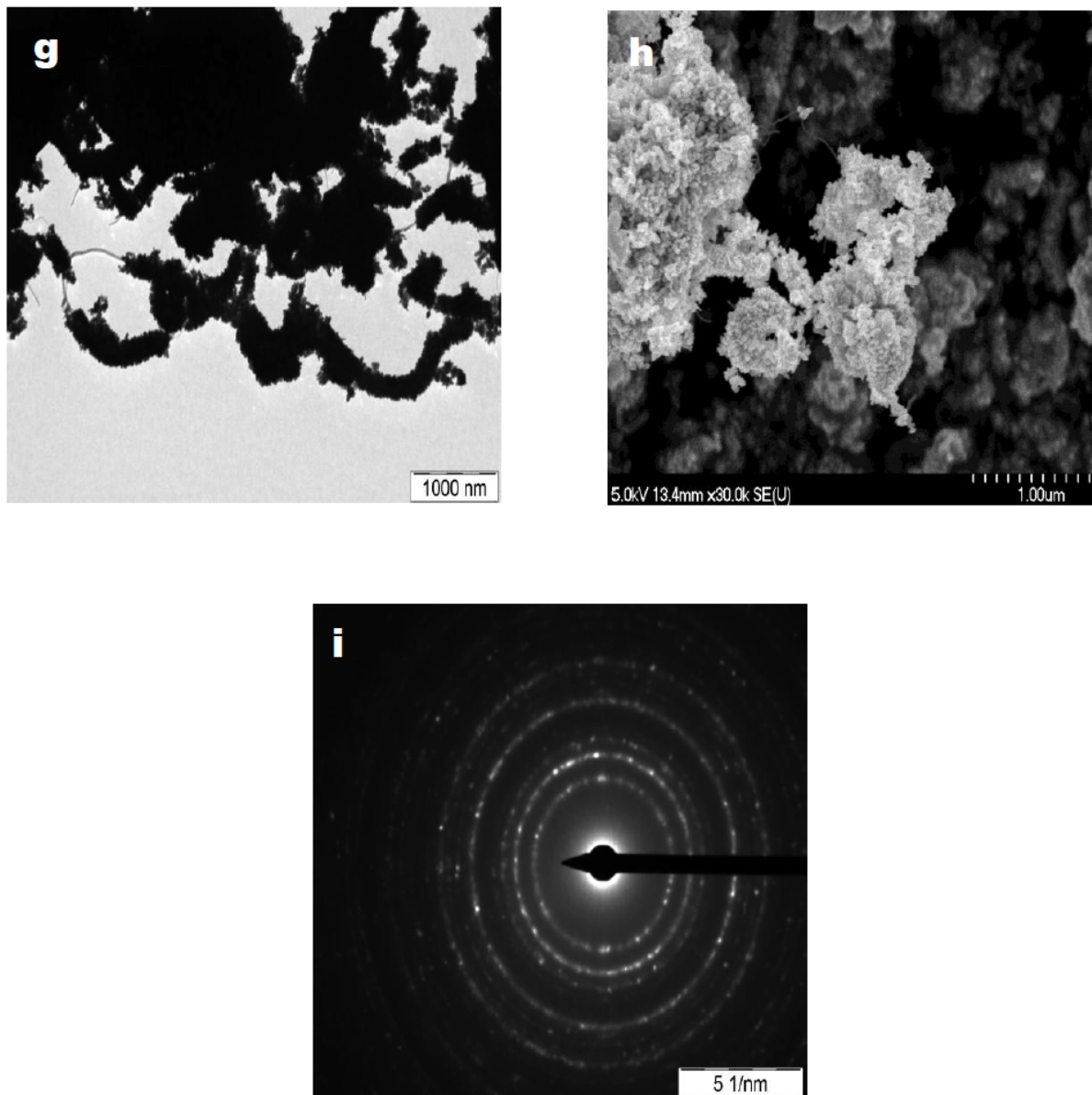


**Figure 4:** TEM and SEM images of SnO<sub>2</sub>/MWNT nanocomposite prepared by the hydrothermal synthesis in water. (a, b) with MWCNT/SnO<sub>2</sub> ratio of 1:4. (c, d) with MWCNT/SnO<sub>2</sub> ratio of 1:8. (e) with MWCNT/SnO<sub>2</sub> ratio of 1:16. (f) with MWCNT/SnO<sub>2</sub> ratio of 1:32. (g-i) with MWCNT/SnO<sub>2</sub> ratio of 1:64.

In aqueous solution, the fabrication of SnO<sub>2</sub>/MWCNT nanocomposite was also successful. EM images clearly revealed (Figure 4) the majority of MWCNTs were covered with SnO<sub>2</sub> nanocrystallites. Increasing the weight ratio from 1:4 to 1:32 the emerging tin-dioxide coverage becomes thicker and thicker (Figure 4). The samples were not consisted of separated inorganic nanocrystallites. Consequently, adhesion of the SnO<sub>2</sub> particles on the surface of MWCNTs was the preferred process. Reaching the weight ratio of 1:64 (Figures 4g and h) the structure of the obtained nanocomposite has shown a high degree of similarity with the sample prepared in ethanol (Figures 3i-k). Although in these cases MWCNTs were almost fully covered, segregated inorganic crystallites were also found during analysis of EM

images. Figure 4i electron diffraction (ED) image shows that SnO<sub>2</sub> particles on the surface of MWCNTs were crystalline.

### 3.2. Raman and FT-IR Investigation

Raman spectroscopic investigation (Figure 5) confirmed the presence of SnO<sub>2</sub> and MWCNT in the samples. Compared to the Raman spectra of pristine MWCNT and Raman spectra of the products exhibits two peaks at 560 cm<sup>-1</sup> and 630 cm<sup>-1</sup> which are characteristic peaks of SnO<sub>2</sub> [27, 28]. The most intensive A<sub>1g</sub> mode of SnO<sub>2</sub> is present in every SnO<sub>2</sub> containing sample. In case of SnO<sub>2</sub> reference A<sub>1g</sub> vibration mode is at 626 cm<sup>-1</sup> while that is at 620 cm<sup>-1</sup> and 622 cm<sup>-1</sup> in case of MWCNT/SnO<sub>2</sub> 1:4 ethanol and MWCNT/SnO<sub>2</sub> 1:4

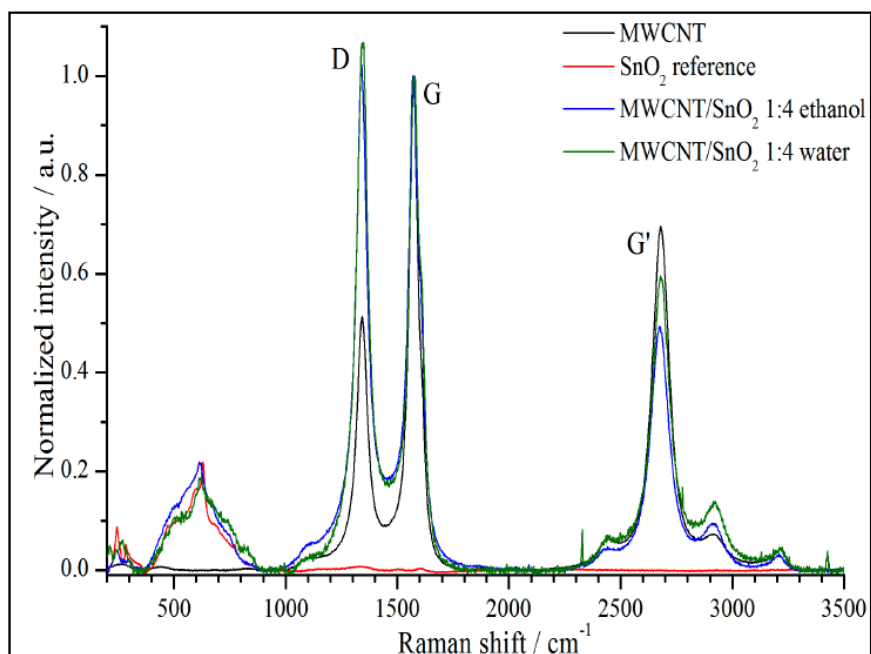


**Figure 5:** Raman spectra of composite samples.

water, respectively. Probably due to the interaction between the MWCNTs and SnO<sub>2</sub> nanoparticles the bands slightly shifted. D, G and G' peaks are the main features of MWCNT Raman spectra. The purity of the MWCNT samples can be easily determined by the ratios of these three peaks (Table 1). The peak intensity ratios in case of MWCNT indicate good quality and highly graphitic nature. Intensities change of MWCNT/SnO<sub>2</sub> 1:4 ethanol and MWCNT/SnO<sub>2</sub> 1:4 water can be assigned to bonding changes with formation of SnO<sub>2</sub> coverage on MWCNTs.

**Table 1:** Summary of the Ratios of the D, G and G' Peaks

	Pristine MWCNT	MWCNT/SnO <sub>2</sub> 1:4 ethanol	MWCNT/SnO <sub>2</sub> 1:4 water
I <sub>D</sub> /I <sub>G</sub>	0.51	1.02	1.07
I <sub>G'</sub> /I <sub>G</sub>	0.70	0.49	0.60
I <sub>G</sub> /I <sub>D</sub>	1.35	0.48	0.56

The presumption that chemical bond formed between MWCNT and SnO<sub>2</sub> during the impregnation process was confirmed by FT-IR analysis. Beside the reference MWCNT (a) SnO<sub>2</sub> (b), and the IR spectra of the (MWCNT/SnO<sub>2</sub>/1:4/EtOH/hydrothermal) composite samples (c) are shown in Figure 6, in the range of 1100 and 400 cm<sup>-1</sup>. Peaks at 495 cm<sup>-1</sup> (Figure 6a), 450 cm<sup>-1</sup> and 600 cm<sup>-1</sup> (Figure 6b) indicate the characteristic bonds of MWCNT and SnO<sub>2</sub>.

As can be seen on the spectrum of the composite a new peak appears about 430 cm<sup>-1</sup> (marked by arrow on Figure 6). It can be assumed that this band (430 cm<sup>-1</sup>) originated from the interaction of the tin-dioxide and the oxygen containing surface functional groups of carbon nanotube while there are

no characteristic peaks of the MWCNT and the SnO<sub>2</sub> in this region.

### 3.3. Surface Area Measurement (BET)

For the widespread characterization of newly prepared materials it is essential to know the specific surface areas. Surface area measurements on obtained powders were determined by gas adsorption using the Brunauer—Emmett—Teller (B.E.T.) equation. Specific surface area of the as-prepared nanocomposites were measured which are we plan to apply in further catalytic and gas sensor applications. Samples were measured are shown in the Table 2 below. Surface area of the applied MWCNTs was 182 m<sup>2</sup>/g. Surface area of the samples were uniformly lower 100m<sup>2</sup>/g as can be seen in Table 2.

### 3.4. Heat Treatment, Crystal Structure Analysis

In order to transform the amorphous inorganic coatings into a crystalline phase the composite samples were heat treated at 450°C for 3 hours. This temperature was low enough to prevent burning of CNTs (burn threshold is around 500°C in the presence of air). EM observations indicated that different quality of coverages can be obtained using different preparation methods. The morphology of the resulted SnO<sub>2</sub> crystallites depends on the preparation method and conditions. After the heat treatment the surface natures are not changed significantly.

The crystallization of the SnO<sub>2</sub>/MWCNTs composite samples with components ratio from 1:4 to 1:64 takes place adequately; therefore only one XRD pattern (Figure 6a) is presented here.

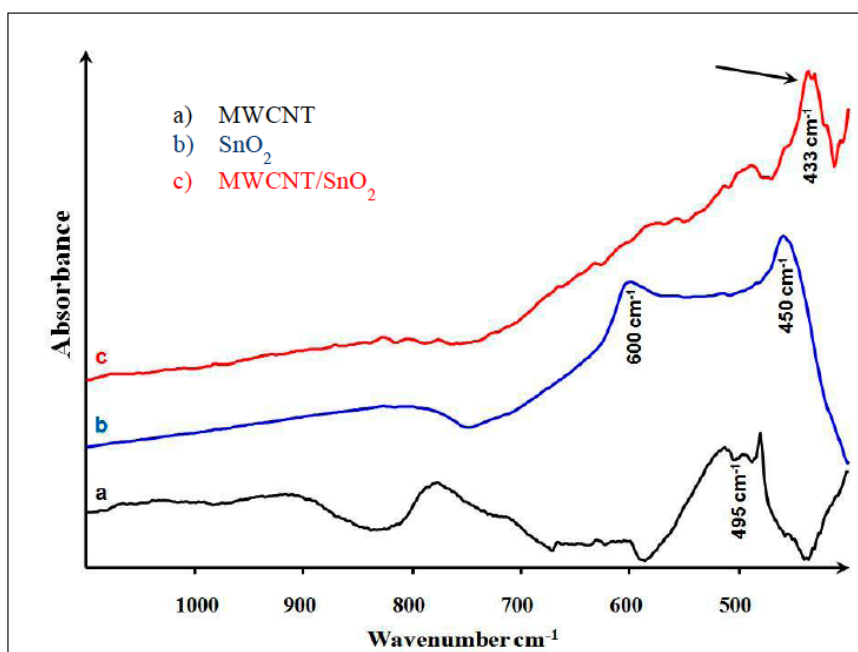


**Figure 6:** IR spectra of composite sample (c) prepared the hydrothermal synthesis in EtOH; and of starting MWCNT (a) and of SnO<sub>2</sub> (b).

**Table 2:** Summary of Surface Areas of As-Prepared SnO<sub>2</sub>/MWCNT Nanocomposites

	H <sub>2</sub> O	EtOH
MWCNT/SnO <sub>2</sub> – 1:16 (impregnation)	76 m <sup>2</sup> /g	63 m <sup>2</sup> /g
MWCNT/SnO <sub>2</sub> – 1:32 (impregnation)	42 m <sup>2</sup> /g	32 m <sup>2</sup> /g
MWCNT/SnO <sub>2</sub> – 1:16 (hydrothermal)	48 m <sup>2</sup> /g	40 m <sup>2</sup> /g
MWCNT/SnO <sub>2</sub> – 1:32 (hydrothermal)	52 m <sup>2</sup> /g	47 m <sup>2</sup> /g
MWCNT/SnO <sub>2</sub> – 1:64 (hydrothermal)	57 m <sup>2</sup> /g	52 m <sup>2</sup> /g

The diffraction peaks at around 33.8°, 37.9° and 51.8° are due to the diffraction at the (101), (200) and (211) planes of SnO<sub>2</sub>, respectively. It is difficult to detect the characteristic peaks of MWCNTs from both XRD patterns because of peak of SnO<sub>2</sub> (110) and the main peak of MWCNTs (002) were overlapped. Furthermore, according to Figure 6a, the average crystallite size can be estimated by Scherrer's formula:  $D = K\lambda/\beta\cos\theta$ ; where D is the grain diameter, K (0.89) is the shape factor,  $\lambda$  is the X-ray wavelength of the Cu K $\alpha$  radiation (0.154 nm),  $\theta$  is the Bragg angle, and  $\beta$  is the experimental full-width half maximum (FWHM) of the respective diffraction peak. The calculated average size of SnO<sub>2</sub> nanocrystallite was about 11-12 nm in the case of hydrothermal synthesis. Using impregnation technique the average size of SnO<sub>2</sub> nanocrystallite was determined as about 8 nm. It means that the as-prepared SnO<sub>2</sub> nanocrystallites aggregated to larger crystallites during hydrothermal synthesis using ethanol as solvent which can be seen on the EM images too.

In order to characterize the quality of tin dioxide coating on the surface of MWCNTs, we performed energy dispersive X-ray analysis (EDX) in the SEM instrument for each

preparation method. Since EDX spectra showed a high degree of similarity only one EDX spectrum is presented (Figure 6b). The most significant signals originate from carbon (C) oxygen (O) and tin (Sn) which proves the components of the nanocomposite samples.

### 3.5. Photocatalytic Efficiency

Photocatalytic efficiencies were determined only for SnO<sub>2</sub>/MWCNT nanocomposites synthesized via hydrothermal method (both H<sub>2</sub>O and EtOH solvents; weight ratio of MWCNT:SnO<sub>2</sub> were 1:4, 1:8, 1:16, 1:32) since this method provided more homogeneous and more uniform coverage. Before photocatalytic measurements, blank experiments were carried out to determine the adsorption capacity of laboratory-prepared nanocomposites. Results pointed out that nanocomposites produced via the utilization of H<sub>2</sub>O solvent during the synthesis method resulted in much higher adsorption ability. These materials adsorbed 10-15 % of phenol at applied concentration after 120 min. in dark, while nanocomposites produced in EtOH solution adsorbed only 1-4 % of phenol. The estimated high difference in adsorption capacities can not be connected to the specific surface areas,

since these properties of the materials are very similar (see Table 2). The difference probably due to some unclarified special surface property, resulted by the different solvents applied in the synthesis methods. The concentration was followed also in case of irradiation without any photocatalyst and the phenol transformation was below 2% during 120 min long irradiation.

Despite the high adsorption capacity, the SnO<sub>2</sub>/MWCNT composites produced in H<sub>2</sub>O solution did not show any photocatalytic efficiency. The nanocomposites synthesized in EtOH solutions showed measurable, but not remarkable

photocatalytic efficiency in comparison with a frequently used, conventional photocatalyst: Aeroxide P25 TiO<sub>2</sub>. Results are showed on Figure 8. While by Aeroxide P25 photocatalyst, 88% of phenol was decomposed after 30 minutes of irradiation, by SnO<sub>2</sub>/MWCNT nanocomposites only 6-11% of phenol was degraded after 120 minutes of irradiation. The differences of photocatalytic efficiencies of different laboratory-prepared nanocomposites (with increasing SnO<sub>2</sub> content) are not significant. The estimated very low photocatalytic efficiency is in contrast with the result described by Wang *et al.* [26]. Authors estimated very high photocatalytic efficiency for SnO<sub>2</sub>/MWCNT nanocomposites

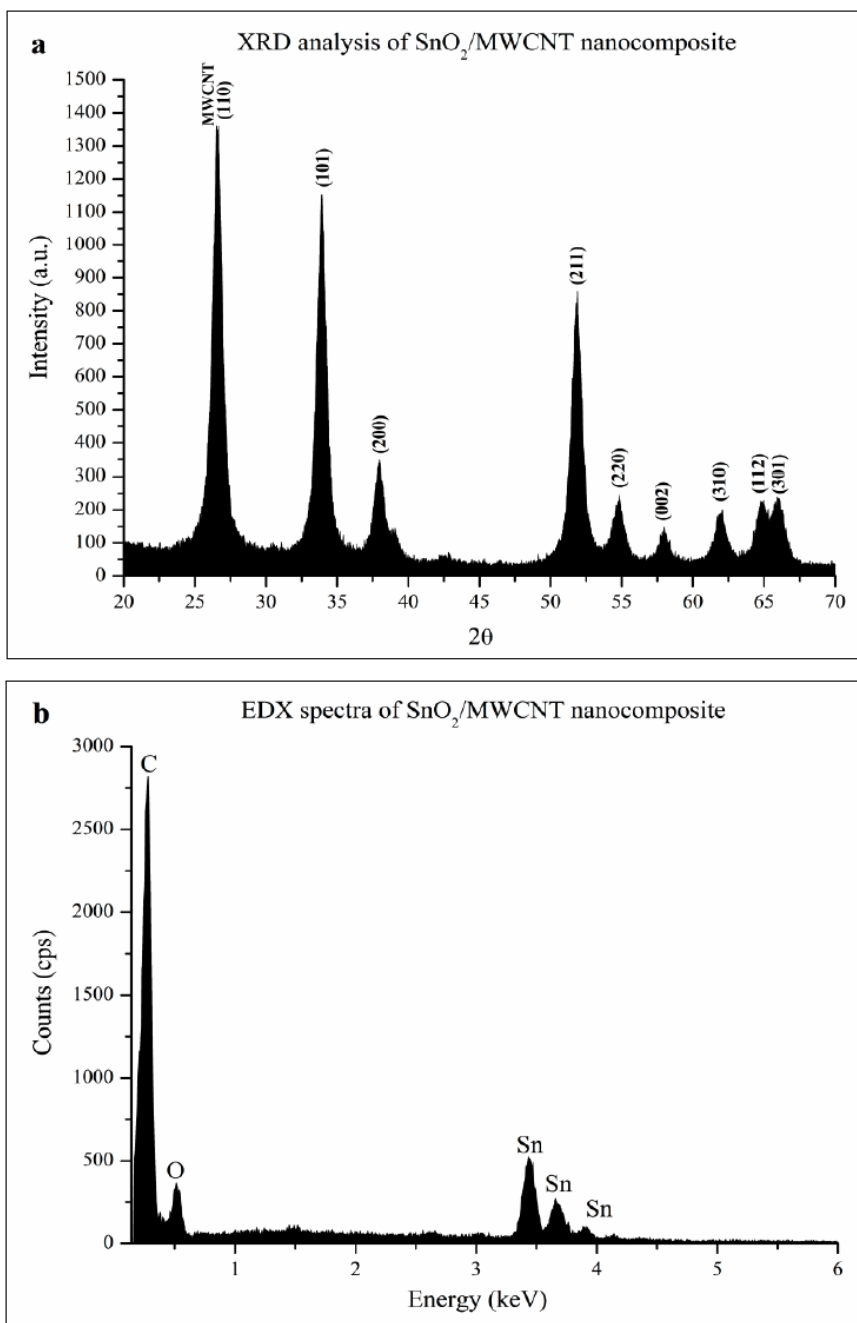


**Figure 7:** XRD (a) and EDX (b) analysis of SnO<sub>2</sub>/MWCNT nanocomposite materials. (a) MWCNT/SnO<sub>2</sub> – 1:4 hydrothermal method. (b) MWCNT/SnO<sub>2</sub> – 1:8 hydrothermal method.

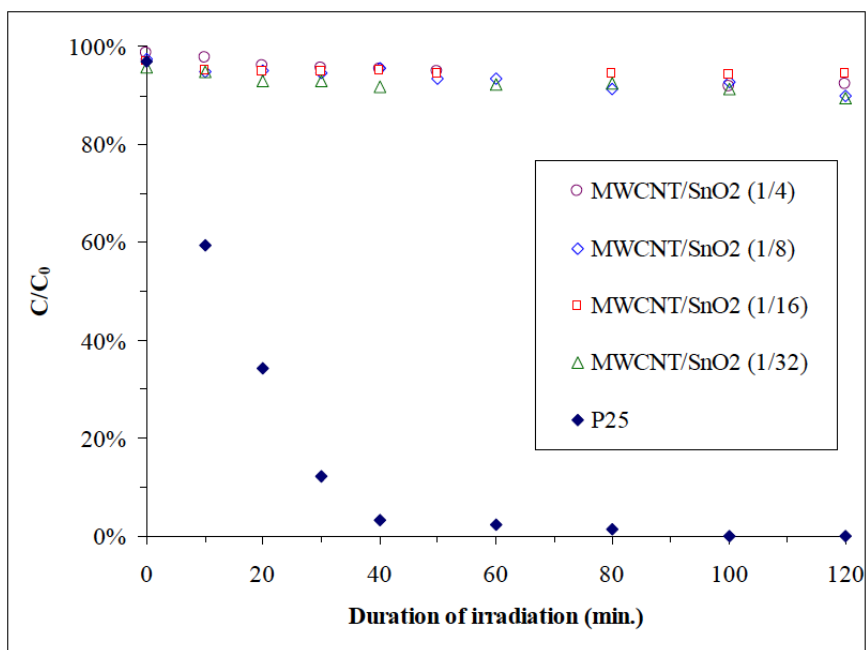


Figure 8: Photocatalytic decomposition of phenol solution ( $V = 100 \text{ mL}$ ;  $c_{\text{phenol}} = 0.1 \text{ mM}$ ) under UV irradiation ( $\lambda_{\text{max}}$  at 365 nm).

(higher than for Aeroxide P25). It should be noted, that in the mentioned paper authors used different type of synthesis method, another model contamination (methyl orange), and the applied irradiation was also a difference. Authors used Philips UV lamp with a wavelength of 254 nm, which could fully photoexcite the electron between the band gap of  $\text{SnO}_2$ . In comparison, in our experiments the UV lamp has an intensity maximum at 365 nm, and emits UV photons only above 300 nm (Figure 9). The band gap of  $\text{SnO}_2$  ( $E_g = 3.6 \text{ eV}$ ) means that it can be excited only by the emitted UV photons below 344 nm, while Aeroxide P25 consist anatase

and rutile phased  $\text{TiO}_2$  as well, so it can be excited by photons below 410 nm. These details can explain the difference of estimated photocatalytic efficiency. Based on our, and Wang and co-workers results it can be concluded  $\text{SnO}_2/\text{MWCNT}$  nanocomposites can be highly effective in an artificial UV (254 nm) light source applying water treatment technology. However, in a Solar irradiation based technology, other photocatalysts (with lower band gap energy; e.g. titanium dioxide based photocatalysts) could be more preferable, since solar spectra consist photons only above 300 nm at sea level.

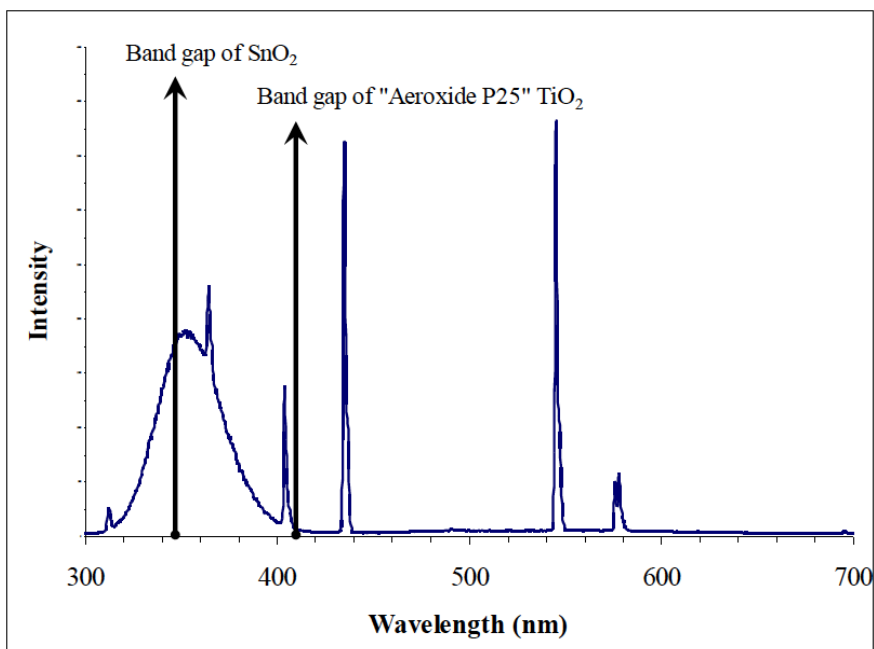


Figure 9: Emission spectra of the applied UV irradiation.

#### 4. CONCLUSION

We studied the synthesis of tin dioxide covered MWCNT based nanocomposite materials using two different preparation methods such as impregnation and hydrothermal. It can be concluded that these synthesis ways were successful in every case but the homogeneity, structure and the thickness of the layers were different. Using various electron microscopy techniques it was verified that different layer construction and morphology can be obtained by varying the applied synthesis techniques.

Raman spectra and XRD measurements confirmed the presence of SnO<sub>2</sub> nanocrystallites on the surface of MWCNT furthermore a real chemical bond formed was confirmed between the MWCNT and SnO<sub>2</sub> nanocrystallites by FT-IR measurements. This statement it could be important during further applications.

The SnO<sub>2</sub> content of the composites was investigated by changing the mass ratio of SnCl<sub>2</sub>·2H<sub>2</sub>O to MWCNT in the case of impregnation and hydrothermal methods in order to produce the most promising SnO<sub>2</sub>/MWCNT nanocomposites for gas sensing technology and photocatalytic applications.

Using impregnation surface of MWCNTs is not completely covered with SnO<sub>2</sub> nanoparticles while in the case of hydrothermal synthesis fully homogeneous coatings formed. The differences observed between the two types of nanocomposites could be explained the disparity of nanocrystallites size of SnO<sub>2</sub>. Products of impregnation method would be ideal candidate as starting material in photocatalytic measurements due to the partially covered MWCNTs which are involved the adsorption process during photocatalysis. The results made it clear that the best wrappings were obtained using hydrothermal synthesis. The most advantage of the hydrothermal method is that by changing the concentration of the reactant and the applied solvents, we can easily control the coverage of SnO<sub>2</sub> nanoparticles on the surface of MWCNTs.

Using EtOH and H<sub>2</sub>O as solvents, SnO<sub>2</sub> nanoparticles with different morphologies can be observed during EM investigations. It can be concluded that the larger weight ratios are more favourable to the adhesion of the inorganic particles in all cases. The best wrappings for the further applications were obtained using hydrothermal synthesis with 1:32 and 1:64 weight ratios. We think that the present approaches here provide good strategies for controllable fabrication of SnO<sub>2</sub>/MWCNT nanocomposites which might have potential applications in the gas sensor or other areas.

The synthesized SnO<sub>2</sub>/MWCNT nanocomposites have low photocatalytic efficiencies in case of UV irradiation at generally used conditions (when  $\lambda > 300$  nm).

#### ACKNOWLEDGEMENTS

The work was supported by the Swiss Contribution SH/7/2/20. Zoltán Németh and Gábor Veréb are grateful for

the financial support of the European Union and the State of Hungary (TÁMOP 4.2.4. A/2-11-1-2012-0001 'National Excellence Program').

#### REFERENCES

- [1] Iijima S. Helical microtubules. *Nature* 1991; 354: 56-8. <http://dx.doi.org/10.1038/354056a0>
- [2] Chu H, Wei L, Cui R, Wang J, Li Y. Carbon nanotubes combined. *Coord Chem Rev* 2010; 254: 1117-34. <http://dx.doi.org/10.1016/j.ccr.2010.02.009>
- [3] Frank S, Poncharal P, Wang ZL, Heer WA. Carbon nanotube quantum resistors. *Science* 1998; 280: 1744-6. <http://dx.doi.org/10.1126/science.280.5370.1744>
- [4] Liu YL, Yang HF, Yang Y, Liu ZM, Shen GL, Yu RQ. Gas sensing. *Thin Solid Films* 2006; 497: 355-60. <http://dx.doi.org/10.1016/j.tsf.2005.11.018>
- [5] Dong H, Lu K. Attaching titania. *Int J Appl Ceram Technol* 2009; 6: 216-22. <http://dx.doi.org/10.1111/j.1744-7402.2008.02270.x>
- [6] Diao P, Liu Z. Electrochemistry. *J Phys Chem B* 2005; 109: 20906-13. <http://dx.doi.org/10.1021/jp052666r>
- [7] Jiang G, Zheng X, Wang Y, Li T, Sun X. Photodegradation. *Powder Technol* 2011; 207: 465-9. <http://dx.doi.org/10.1016/j.powtec.2010.11.029>
- [8] Kauffman DR, Tang Y, Kichambare PD, Jackovitz JF. Long-term performance. *Energy Fuels* 2010; 24: 1877-81. <http://dx.doi.org/10.1021/ef100013v>
- [9] Landi BJ, Ganter MJ, Cress CD, Dileo RA, Raffaella RP. Carbon nanotubes. *Science* 2008; 2: 638-54.
- [10] Han W, Zettl A. Coating. *Nano Letters* 2003; 3(5): 681-3. <http://dx.doi.org/10.1021/nl034142d>
- [11] Kuang Q, Li SF, Xie ZX, Lin SC, Zhang XH, Xie SY, Huang RB, Zheng LS. Controllable fabrication. *Carbon* 2006; 44: 1166-72. <http://dx.doi.org/10.1016/j.carbon.2005.11.001>
- [12] Liu YL, Yang HF, Yang Y, Liu ZM, Shen GL, Yu RQ. Gas sensing properties. *Thin Solid Films* 2006; 497: 355-60. <http://dx.doi.org/10.1016/j.tsf.2005.11.018>
- [13] Du G, Zhong C, Zhang P, Guo Z, Chen Z, Liu H. Tin dioxide/carbon nanotube. *Electrochim Acta* 2010; 55: 2582-6. <http://dx.doi.org/10.1016/j.electacta.2009.12.031>
- [14] Pang HL, Lu JP, Chen JH, Huang CT, Liu B, Zhang XH. Preparation of SnO<sub>2</sub>. *Electrochim Acta* 2009; 54: 2610-5. <http://dx.doi.org/10.1016/j.electacta.2008.10.058>
- [15] Feng C, Li L, Guo Z, Li H. Synthesis and characterization. *J Alloys Compd* 2010; 504: 457-61. <http://dx.doi.org/10.1016/j.jallcom.2010.05.144>
- [16] Noerochim L, Wang JZ, Chou SL, Li HJ, Liu HK. SnO<sub>2</sub> coated. *Electrochim Acta* 2010; 56: 314-20. <http://dx.doi.org/10.1016/j.electacta.2010.08.078>
- [17] Xu C, Sun J, Gao L. Synthesis of multiwalled carbon nanotubes. *J Phys Chem C* 2009; 113: 20509-13. <http://dx.doi.org/10.1021/jp909740h>
- [18] Zhu CL, Zhang ML, Qiao YJ, Gao P, Chen YJ. High capacity. *Mater Res Bull* 2010; 45: 437-41. <http://dx.doi.org/10.1016/j.materresbull.2009.11.011>
- [19] Du N, Zhang H, Chen BD, Ma XY, Huang HH, Tu JP, Yang DR. Synthesis of polycrystalline SnO<sub>2</sub>. *Mater Res Bull* 2009; 44: 211-5. <http://dx.doi.org/10.1016/j.materresbull.2008.04.001>
- [20] Aroutiounian VM, Arakelyan VM, Khachatryan EA, Shahnazaryan GE, Aleksanyan MS, Forro L, Magrez A, Hernadi K, Nemeth Z. Manufacturing and investigations. *Sens Actuators B* 2012; 173: 890-6. <http://dx.doi.org/10.1016/j.snb.2012.04.039>
- [21] Aroutiounian VM, Adamyan AZ, Khachatryan EA, Adamyan ZN, Hernadi K, Pallai Z, Nemeth Z, Forro L, Magrez A, Horvath E. Study of the surface-ruthenated. *Sens Actuators B* 2013; 177: 308-15. <http://dx.doi.org/10.1016/j.snb.2012.10.106>
- [22] Wu SS, Cao HQ, Yin SF, Liu XW, Zhang XR. Amino acid-assisted hydrothermal synthesis. *J Phys Chem C* 2009; 113: 17893-8. <http://dx.doi.org/10.1021/jp9068762>
- [23] Dimitrov M, Tsoncheva T, Shao S, Kohn R. Novel preparation. *Appl Catal B* 2010; 94: 158-65. <http://dx.doi.org/10.1016/j.apcatb.2009.11.004>

- [24] Linsebigler AL, Lu G, Yates JT. Photocatalysis. *Chem Rev* 1995; 95: 735-58.  
<http://dx.doi.org/10.1021/cr00035a013>
- [25] Sun Y, Wilson SR, Schuster DI. High dissolution. *J Am Chem Soc* 2001; 123: 5348-9.  
<http://dx.doi.org/10.1021/ja0041730>
- [26] Wang N, Xu J, Guan L. Synthesis. *Mater Res Bull* 2011; 46: 1372-6.  
<http://dx.doi.org/10.1016/j.materresbull.2011.05.014>
- [27] Couteau E, Hernadi K, Seo JW, Thien-Nga L, Miko Cs, Gaal R, Forro L. CVD synthesis. *Chem Phys Lett* 2003; 378: 9-13.  
[http://dx.doi.org/10.1016/S0009-2614\(03\)01218-1](http://dx.doi.org/10.1016/S0009-2614(03)01218-1)
- [28] Magrez A, Seo JW, Miko Cs, Hernadi K, Forro L. Growth of carbon nanotubes. *J Phys Chem B* 2005; 109: 100087-91.
- [29] Aroutiounian VM, Arakelyan VM, Khachaturyan EA, Shahnazaryan GE, Aleksanyan MS, Forro L, Magrez A, Hernadi K, Nemeth Z. Manufacturing. *Sens Actuators B* 2012; 173: 890-6.  
<http://dx.doi.org/10.1016/j.snb.2012.04.039>
- [30] Horrillo MC, Serventi A, Rickerby D, Gutiérrez J. Influence of tin oxide. *Sens Actuators B* 1999; 58: 474-7.  
[http://dx.doi.org/10.1016/S0925-4005\(99\)00106-9](http://dx.doi.org/10.1016/S0925-4005(99)00106-9)
- [31] Mandayo GG, Castano E, Gracia FJ, Cirera A, Cornet A, Morante JR. Strategies. *Sens Actuators B* 2003; 95: 90-6.  
[http://dx.doi.org/10.1016/S0925-4005\(03\)00413-1](http://dx.doi.org/10.1016/S0925-4005(03)00413-1)